Title	Numerical and experimental studies on circulation of working fluid in liquid droplet radiator
Author(s)	Totani, Tsuyoshi; Kodama, Takuya; Watanabe, Kensuke; Nanbu, Kota; Nagata, Harunori; Kudo, Isao
Citation	Acta Astronautica, 59(1-5), 192-199 https://doi.org/10.1016/j.actaastro.2006.02.034
Issue Date	2006-07
Doc URL	http://hdl.handle.net/2115/14525
Type	article (author version)
Note	Space for Inspiration of Humankind, Selected Proceedings of the 56th International Astronautical Federation Congress, Fukuoka, Japan, 17-21 October 2005
File Information	Fullpaper_short_hr.pdf

Instructions for use

IAC-05-C2.6.04

NUMERICAL AND EXPERIMENTAL STUDIES ON CIRCULATION OF WORKING FLUID IN LIQUID DROPLET RADIATOR

Tsuyoshi Totani, Takuya Kodama, Kensuke Watanabe, Kota Nanbu, Harunori Nagata and Isao Kudo

Hokkaido University, Sapporo, Japan

E-mail: tota@eng.hokudai.ac.jp

ABSTRACT

A model of the circulation of the working fluid in a liquid droplet radiator has been developed.   The model is based on Bernoulli's law and the loss of the hydraulic head.   The behavior of the circulation of the working fluid calculated from the model is compared with that obtained from experiments in the case that the flow rate of the circulating working fluid is changed.   In radiators, the flow rate of the circulating working fluid is changed in order to match the change of the waste heat generated in large-space structures.   The flow rates of the circulating working fluid calculated from the model correspond to those obtained from the experiments well.   The circulation mechanism of the working fluid in the liquid droplet radiator has been clarified.   The model developed in the present work will allow us to control the flow rate of the working fluid in the liquid droplet radiator automatically.

INTRODUCTION

Disposing large quantities of waste heat is one of the technical issues that must be considered in order to realize large-space structures (LSSs) that handle high power (from megawatt to gigawatt order) such as space solar power satellites (SPSs).[1,2]   The liquid droplet radiator (LDR) is an important candidate for resolving this issue.   Its lightweight structure, high resistance to meteorite impacts, small storage volume requirement at launch and easy deployment in space make it a very attractive heat removal system for the LSSs.

The operation of an LDR is schematically shown in Fig. 1.   The LDR, which consists of a droplet generator, a droplet collector, a circulating pump, a
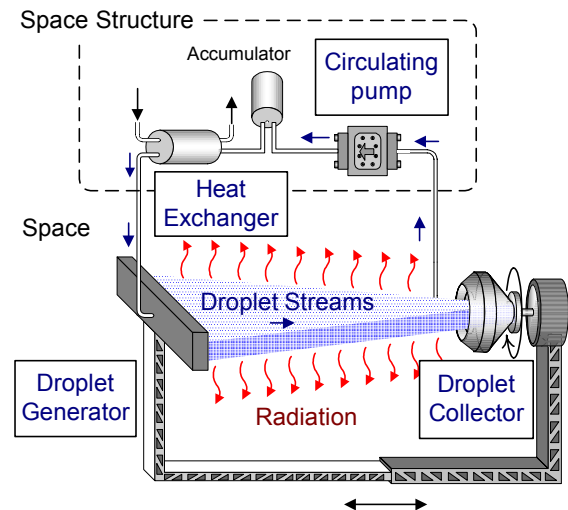

Fig. 1: Schematic diagram of liquid droplet radiator

bellows-type pressure regulator (an accumulator) and a heat exchanger, circulates the working fluid as follows: The working fluid is heated through a heat

exchanger by the waste heat generated in an LSS. Then, the working fluid is emitted into space through nozzles of the droplet generator toward a droplet collector as tiny liquid droplets. During the transport in space from the droplet generator to the droplet collector, the droplets lose thermal energy via radiative heat transfer. After the cooled droplets are captured by the droplet collector, the working fluid is recycled through the accumulator to the heat exchanger by a circulating pump.

Liquids with low vapor pressures are candidates for the working fluids from the viewpoint of minimizing evaporation loss. In the cases of the waste heat temperature range of 250 K - 350 K, of 370 K - 650 K and 500 K - 1000 K, silicone oils, liquid metal eutectics and liquid tin are candidates, respectively.[3] The surface radiating waste heat is the surface of droplets in LDRs. Because LDRs do not require solid bodies to protect the radiating surface from punctures by small particles such as debris or small meteorites, they are lightweight, stored in a small volume at launch and easily deployed in orbit.[4] Taussig and Mattick[4] reported that LDRs can be as much as 5 to 10 times lighter than advanced heat pipe radiators. Massardo et al.[5] reported that the specific mass of a solar power dynamic system with an LDR is 27% less than that with a conventional heat pipe radiator. Droplet generation experiments and droplet collection experiments on earth have been conducted at the NASA Glenn Research Center and the National Institute of Advanced Industrial Science and Technology in Japan.[6-9] Droplet generation experiments and droplet collection experiments under microgravity using drop-shafts have been carried out by the authors.[10, 11]

LDRs change the flow rate of the circulating working fluid in order to correspond to the change in the amount of the waste heat removed from LSSs. The numbers of revolutions of the droplet collector and circulating pump, and the pressure applied on the bellows-type pressure regulator, are controlled in order to change the flow rate of the circulating working fluid. However, few studies have been carried out on controlling the flow rate of the circulating working fluid in the LDR. It has not been clarified how the flow rate of the circulating working fluid in the LDR is controlled.

In this study, a model of the circulation of the working fluid in the LDR is developed. The behavior of the circulation of the working fluid calculated from the model is compared with that obtained from experiments in the case that the flow rate of the circulating working fluid is changed.

EXPERIMENTAL & MODEL

Figure 2 shows a schematic diagram of the experimental setup. Figure 3 shows a photograph of the experimental setup. The working fluid flows in the order of ①②③④⑤⑥⑦①, as indicated in Fig. 2. The volume of the working fluid in the droplet collector ② and the bellows-type pressure regulator ⑤ can change. Two flowmeters ④ and ⑥ are set between ② and ⑤. In the case that the flow rate at ④ is greater than that at ⑥, the volume of the working fluid corresponding to the difference of the flow rates is supplied from ② and stored in ⑤. In the case that the flow rate at ⑥ is greater than that at ④, the working fluid is supplied from ⑤ and is pooled in ②.
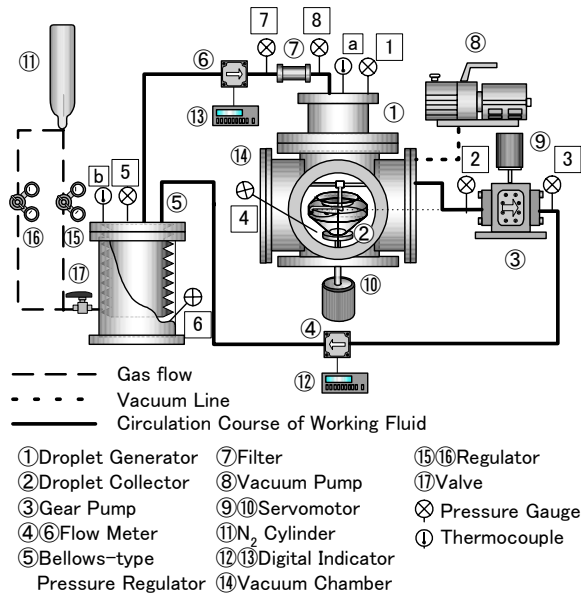
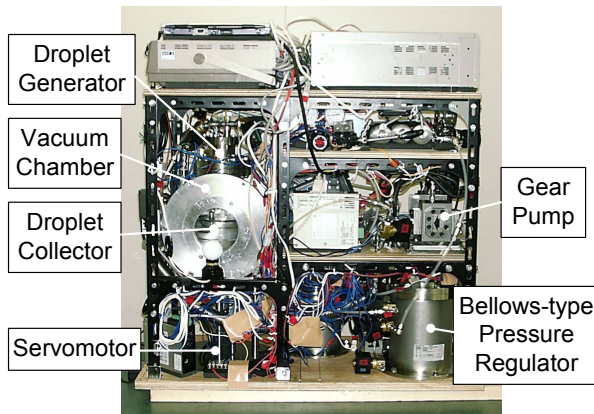Fig. 2: Schematic diagram of experimental setup

— — — Gas flow
• • • • Vacuum Line
——— Circulation Course of Working Fluid

①Droplet Generator ⑦Filter ⑮⑯Regulator
②Droplet Collector ⑧Vacuum Pump ⑰Valve
③Gear Pump ⑨⑩Servomotor ⊗ Pressure Gauge
④⑥Flow Meter ⑪N₂ Cylinder ① Thermocouple
⑤Bellows–type ⑫⑬Digital Indicator
   Pressure Regulator ⑭Vacuum Chamber

Fig. 3: Experimental setup

Fig. 4: Schematic diagram of droplet generator

$$\Delta P = P_1 - P_4$$
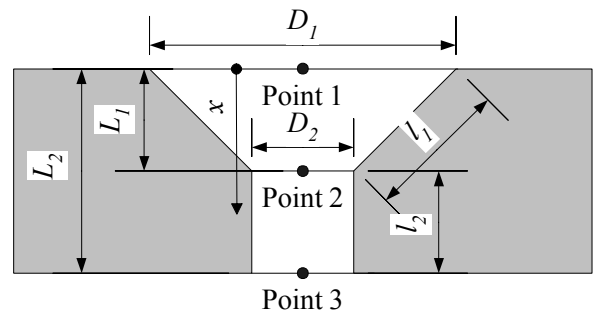
Fig. 5: Details of nozzle in droplet generator

Droplet generator

Figure 4 shows a schematic diagram of the droplet generator. The working fluid, which is pressurized by a bellows-type pressure regulator, is subjected to a pressure disturbance using a piezoelectric vibrator in the droplet generator and then is emitted in the vacuum chamber ⑭ through a single nozzle, as shown in Fig. 4. The pressure disturbance produces radial variation on the surface of the cylindrical jet-shaped working fluid. The
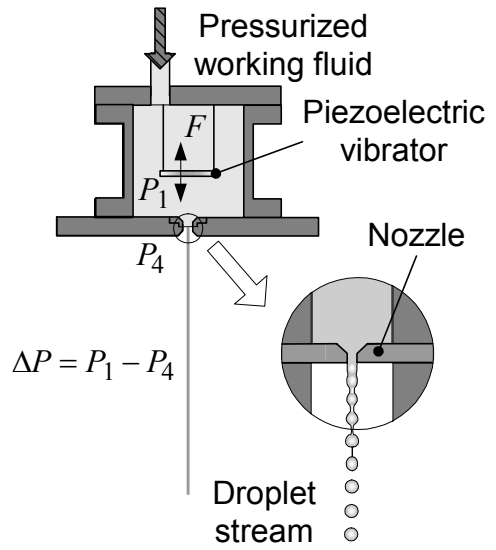
amplitude of this radial variation increases under certain conditions.[12-14] This increase in radial variation causes the working fluid to break up from a jet into tiny droplets. The transformation from a jet to droplets is schematically illustrated in Fig. 4. The velocity u_1 of the working fluid at the exit of the droplet generator is obtained using

$$u_1 = \frac{4}{\pi D_2{}^2} Q , \qquad (1)$$

where Q is the circulation rate of the working fluid in LDR.

Details of the nozzle in the droplet generator are shown in Fig. 5. Considering the friction loss in

the nozzle H_{gf}, the pressure loss in the entrance length of the nozzle H_{ge} and the pressure loss at the inlet of the nozzle H_{gi}, the head loss at the droplet generator H_g is shown as

$$H_g = H_{gf} + H_{ge} + H_{gi} . \qquad (2)$$

The velocity in the nozzle u_g changes with the position x in the nozzle because the sectional area of the nozzle changes with position x. The friction loss in the nozzle H_{gf} is shown with the flow rate Q as

$$H_{gf} = \lambda \frac{L}{D} \frac{u_g{}^2}{2g}$$

$$= \frac{128 \mu Q}{\pi \rho g} \left[\frac{l_1}{3(D_1 - D_2)} \left\{ \frac{1}{D_2{}^3} - \frac{1}{D_1{}^3} \right\} + \frac{l_2}{D_2{}^4} \right], \quad (3)$$

where D_1 ($=1.2 \times 10^{-3}$ m) and D_2 ($=4.0 \times 10^{-4}$ m) are the diameters of the nozzle, as shown in Fig. 5. l_1 ($=5.66 \times 10^{-4}$ m) and l_2 ($=4.0 \times 10^{-4}$ m) are the lengths of the nozzle. μ is the viscosity of the working fluid. Because the Reynolds number in the vinyl tube is sufficiently small, the flow is regarded as laminar and the Darcy friction factor is given by[15]

$$\lambda = \frac{64}{\mathrm{Re}} = \frac{64 \mu}{\rho u D} . \qquad (4)$$

The pressure loss in the entrance length of the nozzle H_{ge} is expressed as

$$H_{ge} = \zeta_{ge} \frac{L}{L_e} \frac{u_g{}^2}{2g}$$

$$= \frac{2 \zeta_i \mu Q}{a \pi \rho g} \left[\frac{l_1}{3\sqrt{2}(D_1 - D_2)} \left\{ \frac{1}{D_2{}^3} - \frac{1}{D_1{}^3} \right\} + \frac{l_2}{D_2{}^4} \right], \quad (5)$$

where L_e is the entrance length of the nozzle, which is given by[16] $L_e = a \, \mathrm{Re} \, D$, a is the coefficient of the entrance length ($=0.065$), and ζ_i is the coefficient of pressure loss in the entrance length ($= 2.7$).[16]

The pressure loss at the inlet of the nozzle H_{gi} is given as

$$H_{gi} = \zeta_i \frac{u_g{}^2}{2g} = \zeta_i \frac{8 Q^2}{g \pi^2 D_2{}^4} , \qquad (6)$$

where ζ_i is the coefficient of loss at the inlet ($= 0.25$).[15]

Droplet collector

The centrifugal collector shown in Fig. 6 has been adopted in this study. The centrifugal collector captures incident droplets at the liquid film inside the spinning cone. The liquid film is formed because incident droplets migrate radially outward due to centrifugal force. The working fluid flows out through stationary pitot tubes immersed in a rotating liquid pool. The working fluid is pushed out by the pressure produced by the centrifugal force and momentum generated by the rotation of the spinning cone.

The streamlines of stable flow in the rotating body are concentric circles on the plane vertical to the rotation axis. As shown in Fig. 7, a pitot tube resides in the rotating working fluid in this droplet collector. The wake flow is generated downstream of the pitot tube. In the case of the centrifugal collectors with small circumferences, the entrance of the pitot tube could be located in the wake flow. In this case, u_e and P_e are shown as,[17]

$$u_e = c \cdot r_e \omega = c \cdot 2 \pi r_e \frac{f}{60} , \qquad (7)$$

$$P_e = P_4 + \frac{1}{2} \rho \left(c \cdot 2 \pi \frac{f}{60} \right)^2 \left(r_e{}^2 - r_i{}^2 \right), \qquad (8)$$

where the constant c is a value specific to the shape and arrangement of the centrifugal collector and the pitot tube ($=0.86$ in this study). r_e and r_i are the
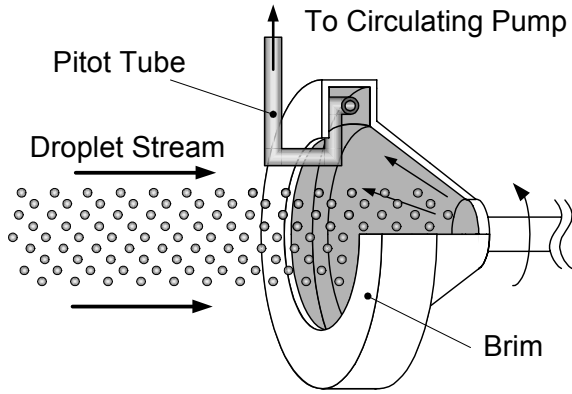
Fig. 6: Schematic diagram of droplet collector

radii of the entrance of the pitot tube ($=8.0 \times 10^{-2}$ m) and the inner surface of the working fluid in the droplet collector, respectively. r_i is chosen in such a way that the volume of the working fluid pressed against the wall because of the rotation of the droplet collector is equal to the volume of the working fluid in the droplet collector ($=7.3 \times 10^{-2}$ m).

Circulating pump

An SK1-213 gear pump (Shimadzu Corporation) was adopted as the circulating pump in the present work because it is small and can push out the working fluid under a large pressure difference between upstream and downstream of the gear pump. A schematic diagram of the gear pump is shown in Fig. 8. The working fluid is pushed out by the revolution of the gears.

The flow rate that the SK1-213 gear pump discharges is given as

$$Q = U_{th} \frac{N}{60} - \frac{A_{gp}}{\mu}(P_3 - P_2), \qquad (9)$$

where U_{th} is the theoretical discharge rate per rotation of the gears ($=1$ ml/rev.) and N is the revolution of the gears per minute. As shown in Fig. 8, there is a clearance between each gear and
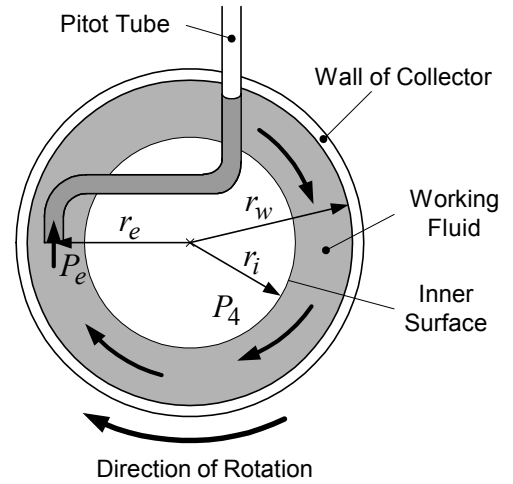

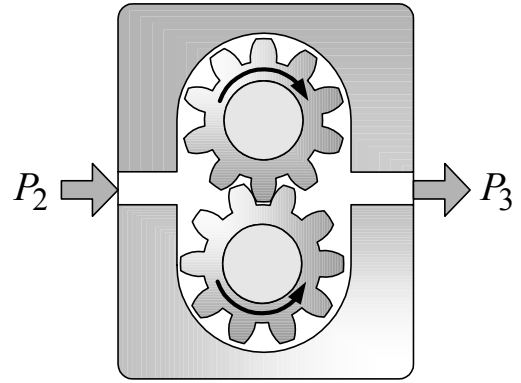Fig. 7: Top-view schematic diagram of centrifugal collector from top view

Fig. 8: Schematic diagram of gear pump

the outside case of the gear pump because of self-lubrication and the rotation of the gear. The second term on the right-hand side of Eq. (9) indicates the flow rate of the working fluid returning from downstream to upstream of the gear pump through the clearance. A_{gp} is a constant and decreases as the number of revolutions decreases. By transforming Eq. (9), the hydraulic head generated at the gear pump ③ is obtained using

$$\Delta H_{gp} = \frac{P_3 - P_2}{\rho g} = -\frac{\mu}{\rho g A_{gp}}\left(Q - U_{th} \frac{N}{60}\right), \quad (10)$$

where g denotes the gravitational acceleration ($=9.81$ m/s^2) and ρ is the density of the working fluid.
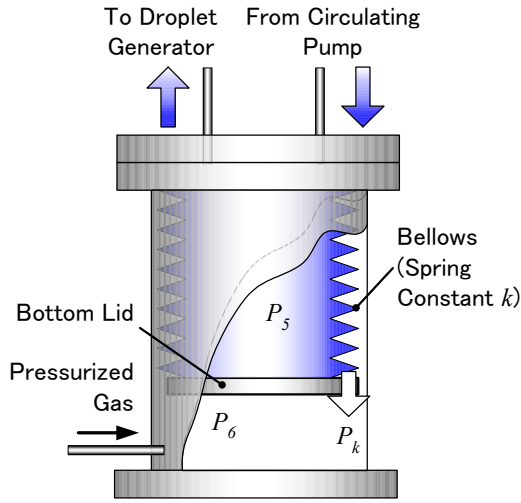
5

Fig. 9: Bellows-type pressure regulator

Bellows-type pressure regulator

The bellows-type pressure regulator has functions of pressurizing the working fluid and flow equalization. The structure of ⑤ is shown in Fig. 9. ⑤ has a bellows that contains the working fluid. The working fluid is pressurized using nitrogen gas from outside of the bellows. The bellows contributes to preventing the working fluid from absorbing the pressurized nitrogen gas. The bellows has a characteristic of a spring. Considering the spring force of the bellows and the pressure of gas outside the bellows, the pressure of the working fluid in ⑤ is given as

$$P_5 = P_6 + \frac{k(z - z_n)}{A_b} , \qquad (11)$$

where k is the spring contact of the bellows (= 3.12 N/mm) and A_b is the area of the bottom lid of the bellows (=1.86×10^{-2} m^2). z is the length of the bellows and z_n is the natural length of the bellows. z is calculated from the difference between the flow rate of inflow to the bellows Q_4 and the flow rate of outflow from the bellows Q_6 using

$$z = z_0 + \frac{(Q_4 - Q_6)\Delta t}{A_b} , \qquad (12)$$

where z_0 denotes the length of the bellows Δt seconds ago.

Filter

A filter is used to remove particles such as dust from the working fluid. Particles such as dust cause the blockade in the nozzle of the droplet generator. An SS-4F-15 filter (Swagelok Company), in which there is a sintered metal element with a nominal gap size of 15 μm, is adopted in this study.

Flow meter

The volume of the working fluid could change in the droplet collector and bellows-type pressure regulator during circulation experiments on the working fluid. Two flowmeters are set between ② and ⑤, and between ⑤ and ②, as shown in Fig. 3. OVAL M-III LSF41C0-M2 (OVAL corporation), which is a displacement meter, is adopted in the flowmeters. A YS02C strainer, with a net mesh gap of 77 μm, is set upstream of the flow meter to remove particles such as dust.

Piping

The hydraulic head lost from the exit of ⑤ to the exit of the droplet generator ① ΔH_{5-1} is shown as

$$\Delta H_{5-1} = (4\zeta_{el} + \zeta_b)\frac{u^2}{2g} + \lambda \frac{L_{5-1}}{D}\frac{u^2}{2g} + \zeta_6 \frac{u_6}{2g} + \zeta_7 \frac{u_7}{2g} + H_g , \qquad (13)$$

where D is the diameter of the piping (=4.35×10^{-3} m) and L_{5-1} is the length of the piping from ⑤ to ① (= 1.45 m). u, u_6 and u_7 are the velocity of the working fluid in the piping and the average velocities of the working fluid in ⑥ including a strainer and in filter ⑦, respectively. ζ_{el} and

ζ_b are the coefficients of loss at an elbow and a bend. The coefficient of loss at the elbow is given as[18]

$$\zeta_{el} = 0.946 \sin^2\left(\frac{\theta}{2}\right) + 2.05 \sin^4\left(\frac{\theta}{2}\right) = 0.986, \quad (14)$$

where ϑ is the angle of the bend (= 90°). The coefficient of loss at the bend is given as[18]

$$\zeta_b = 0.131 + 1.847\left(\frac{D}{2 r_b}\right)^{3.5} = 0.412, \quad (15)$$

where r_b is the radius of curvature. The friction loss in the piping is derived from Eq. (13) as

$$\lambda \frac{L_{5-1}}{D}\frac{u^2}{2g} = \frac{64\mu}{\rho u D}\frac{L_{5-1}}{D}\frac{u^2}{2g} = f\left(\frac{u}{2g}\right). \quad (16)$$

As shown in Eq. (16), the friction loss in the piping is a function of $u/2g$. The pressure losses at ⑥ including a strainer and ⑦ are caused by friction in the strainer and the filter. The pressure losses at ⑥ including a strainer and ⑦ has been assumed to be a function of $u/2g$, as shown in Eq. (16). ζ_6 and ζ_7 are the coefficients of loss at ⑥ including a strainer and ⑦, respectively. Values calculated from experimental data obtained Δt seconds ago are substituted in ζ_6 and ζ_7.

The hydraulic head lost ΔH_{2-5} from ② to the entrance of ⑤ is shown as

$$\Delta H_{2-5} = (4\zeta_{el} + 2\zeta_b)\frac{u^2}{2g} + \lambda \frac{L_{2-5}}{D}\frac{u^2}{2g} + \zeta_4 \frac{u_4}{2g}, \quad (17)$$

where L_{2-5} is the length of the piping from ② to ⑤ (= 2.3 m). u and u_4 are the velocity of the working fluid in the piping and the average velocity of the working fluid in ④ including a strainer, respectively. ζ_4 is the coefficient of loss at ④ including a strainer. The value calculated from

experimental data obtained Δt seconds ago is substituted in ζ_4.

Working fluid

A commercially available silicone oil (Shin-Etsu Chemical Co., Ltd., KF96-50cSt) is employed as the working fluid.

Bernoulli's law

Applying Bernoulli's law and taking the loss of the hydraulic head into account between the exit of ⑤ and the exit of ①, we obtain

$$\frac{u_5^2}{2g} + \frac{P_5}{\rho g} = \frac{u_1^2}{2g} + \frac{P_4}{\rho g} + \Delta h_{5-1} + \Delta H_{5-1}, \quad (18)$$

where u_1 and u_5 are the velocities at the exit of ① and at the exit of ⑤, respectively. P_4 and P_5 are the pressure in ⑭ and the pressure of working fluid in ⑤. Δh_{5-1} is the vertical interval between the exit of ⑤ and the exit of ① (=0.30 m). Applying Bernoulli's law and taking into account the loss of the hydraulic head between ② and ⑤, we obtain

$$\frac{u_e^2}{2g} + \frac{P_e}{\rho g} + \Delta H_{gp} = \frac{u_5^2}{2g} + \frac{P_5}{\rho g} + \Delta h_{2-5} + \Delta H_{2-5},$$

$$(19)$$

where u_5 and P_5 are the velocity and pressure at the entrance of ⑤. Δh_{2-5} is the vertical interval between the entrance of the pitot tube in ② and the entrance of ⑤ (=0.17 m).

The velocities u_4, u_5, u_6 and u_7 are equal to the velocity u because the diameter in ④, the diameter of the piping at the exit of ⑤, the diameter in ⑥ and the diameter in ⑦ are represented by the diameter D (=4.35×10⁻³ m) of the piping. The flow rate Q and velocity u are related through
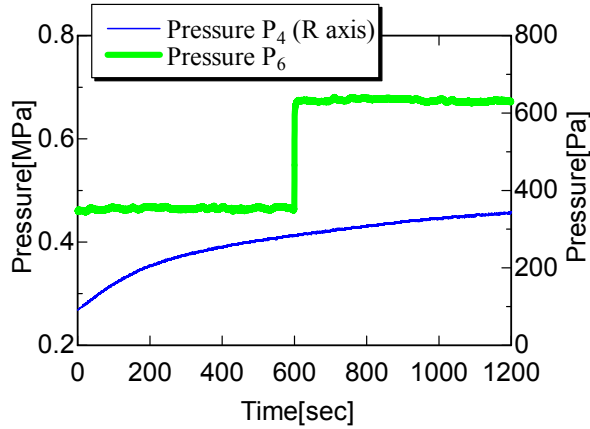
Fig.10   Histories of pressure

Fig.11   Histories of pressure

$$Q = \frac{\pi D^2}{4} u . \tag{20}$$

Solving Eq. (18) for Q, the flow rate between the exit of ⑤ and the exit of ①, namely the flow rate of ⑥ Q_6 is obtained.   Solving Eq. (19) for Q, the flow rate between ② and ⑤, namely the flow rate of ④ Q_4 is obtained.   The pressures P_4 and P_6 are unknown in these equations.   Experimental data is substituted at the pressure P_4 and P_6.   The pressure in ⑭ P_4 correspond to the pressure in space.   The pressure of gas outside ⑤ P_6 can be controlled.

RESULTS AND DISCUSSION

Figures 10 and 11 indicate the histories of pressure P_4 and P_6 in the cases that flow rates are changed from 100 ml/min to 130 ml/min and from 130 ml/min to 100 ml/min, respectively.   These data are substituted in the model described in the preceding section.   Figures 12 and 13 show the histories of flow rates calculated using the model and obtained in the experiments, respectively.   The symbols such as (1) and (2) shown in Figs. 12 and 13 indicate when the numbers of revolutions of the droplet collector and gear pump, and the pressure applied on
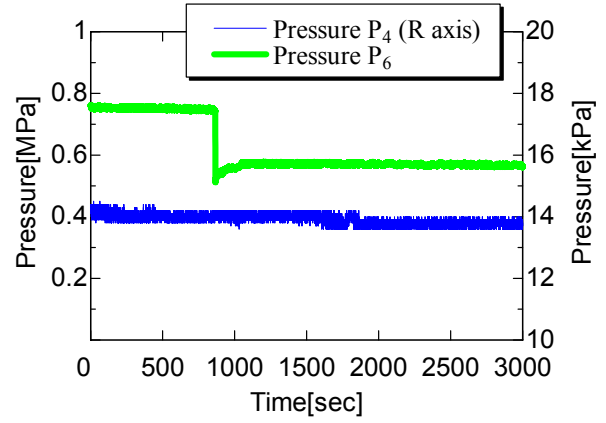
the bellows-type pressure regulator P_6 are adjusted, respectively.   The symbols in Figs. 12 and 13 correspond to the symbols in Tables 1 and 2, respectively.   Tables 1 and 2 indicate the time and values of the parameters after the change.   Both the flow rates of ④ and ⑥ calculated from the model correspond well to those obtained in the experiments. The circulation mechanism of the working fluid in the liquid droplet radiator has been clarified.   It is clear that the model developed in this work can be used to forecast the behavior of the circulation of the working fluid in the LDR.   It appears in Figs. 12 and 13 that the flow rates decrease with time.   The difference in pressure between pressure gauges 7 and 8 increases with time.   ⑦ is located between pressure gauges 7 and 8.   Filters are gradually choked by particles such as dust.   The decrease in the flow rates with time is believed to be due to the choke of the filter.   This phenomenon can be improved by adjusting the numbers of revolutions of the gear pump and droplet collector based on the model developed in this study.   The parameters set in Tables 1 (1) and 2 (2) were preliminarily obtained before the experiments.   The choke of the filter is the reason why adjustments of the flow rates are
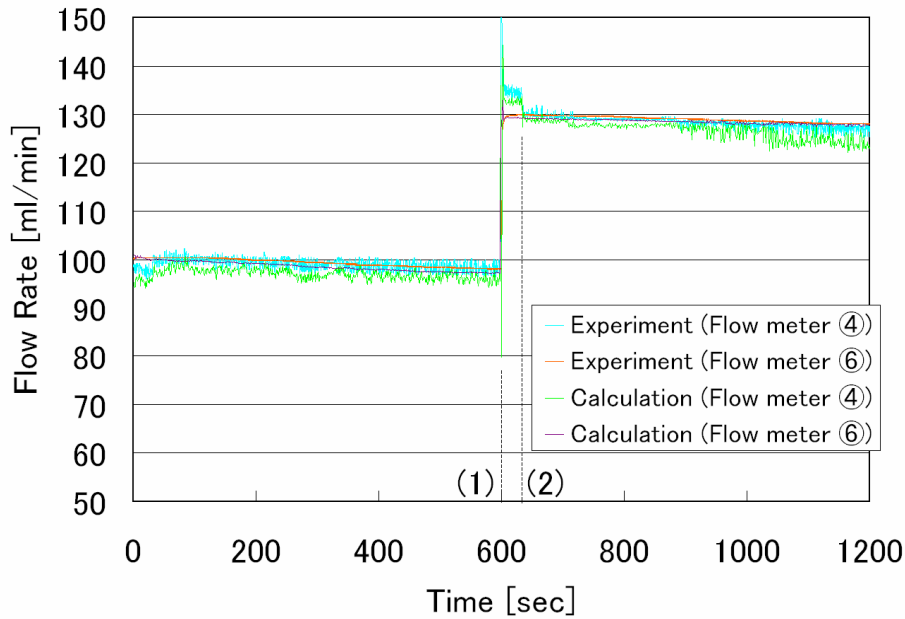
Fig.12   Histories of flow rate

Table 1   Changes in parameters

	Time [sec]	Pressure [MPa]	Rate of revolutions of droplet collector [rpm]	Rate of revolutions of gear pump [rpm]
-	-	0.477	670	193
(1)	599	0.683	720	271
(2)	633	0.683	720	265

needed.

CONCLUSIONS

A model of the circulation of the working fluid in the LDR has been developed.   The flow rates of the circulating working flow calculated from the model correspond well to those obtained from the experiments.   The circulation mechanism of the working fluid in the liquid droplet radiator has been clarified.   The model will allow us to control the flow rate of the working fluid in the liquid droplet radiator automatically.

REFERENCES

1.   Glaser, P. E., "Power from the Sun: Its Future," Science, Vol. 162, 1968, p. 857.

2.   Mankins, J. C., "A Fresh Look at Space Solar Power: New Architectures, Concepts and Technologies," *Acta Astronaoutica*, Vol. 41,
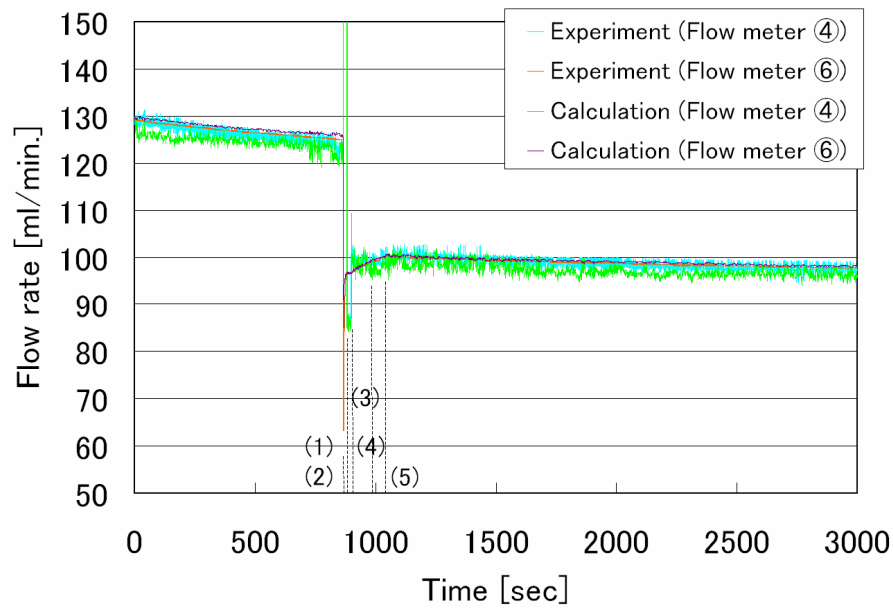
Fig.13 Histories of flow rate

Table 2 Changes in parameters

	Time [sec]	Pressure [MPa]	Rate of revolutions of droplet collector [rpm]	Rate of revolutions of gear pump [rpm]
		0.756	800	283
(1)	865	0.570	670	283
(2)	879	0.570	670	202
(3)	901	0.570	670	217
(4)	990	0.570	670	220
(5)	1040	0.570	670	222

Nos. 4-10, 1997, pp. 347-359

3. Mattick, A. T. and Hertzberg, A., "Liquid Droplet Radiators for Heat Rejection in Space," *Journal of Energy*, Vol. 5, No. 6, 1981, pp. 387-393

4. Taussig, R. T. and Mattick A. T., "Droplet Radiator Systems for Spacecraft Thermal Control," *Journal of Spacecraft and Rockets*, Vol. 23, No. 1, 1986, pp. 10-17

5. Massardo, A. F., Tagliafico, L. A., Fossa, M.

and Agazzani, A., "Solar Space Power System Optimization with Ultralight Radiator," *Journal of Propulsion and Power*, Vol. 13, No. 4, 1997, pp. 560-564

6. Presler, A. F., Coles, C. E., Diem-Kirsop, P. S. and White, K. A., "Liquid Droplet Radiator Program at the NASA Lewis Research Center," ASME 86-HT-15, June 1986

7. White, K. A., "Liquid Droplet Radiator Development Status," AIAA Paper 87-1537,

June 1987

8. Hosokawa, S., Kawada, M., Iwasaki, A. and Kudo, I., "Formation of a Uniform Liquid Droplet Stream for a Liquid Droplet Radiator," *Journal of the Japan Society for Aeronautical and Space Sciences*, Vol. 39, No. 453, 1991, pp. 551-557   (in Japanese)

9. Hosokawa, S., Kawada, M., Iwasaki, A. and Kudo, I., "Observation of Collecting Process of Liquid Droplets in Liquid Droplet Radiator," *Journal of the Japan Society for Aeronautical and Space Sciences*, Vol. 41, No. 474, 1993, pp. 385-390   (in Japanese)

10. Totani, T., Itami, M., Yabuta, S., Nagata, H., Kudo, I., Iwasaki, A. and Hosokawa, S., "Performance of Droplet Emittor for Liquid Droplet Radiator under Microgravity," *Transactions of the Japan Society of Mechanical Engineers B*," Vol. 68, No. 668, 2002, pp. 1166-1173   (in Japanese)

11. Totani, T., Itami, M., Nagata, H., Kudo, I., Iwasaki, A. and Hosokawa, S., "Performance of Droplet Generator and Droplet Collector in Liquid Droplet Radiator under Microgravity," *Microgravity Science and Technology*, Vol. 13, No. 2, 2002, pp. 42-45

12. Rayleigh, L., "On the Instability of a Cylinder of Viscous Liquid under Capillary Force. Philosophical Magazine," Vol. 34, 1892, pp. 130-145

13. Weber, C., "Zum Zerfall eines Flüssigkeitsstrahles, Zeitschrift fuer Angewandte Mathematik und Mechanik," Vol. 11, 1931, pp.136-154

14. Chandrasekhar, "S., Hydrodynamic and Hydromagnetic Stability," Chap. XII, New York, Dover Publications, Inc, 1981

15. F. M. White, Fluid Mechanics, 2nd ed. New York, McGraw Hill, 1999, Chap. 6, 325-426

16. Kiso Ryutai Rikigaku Henshu Iinkai, Kiso Ryutai Rikigaku, (Sangyou Tosho, Tokyo, 1989), Chap.6, 45-58 (in Japanese).

17. Totani, T., Itami, M., Nagata, H., Kudo, I. and Iwasaki, A., "Measurement technique for pumping performance of a centrifugal collector under microgravity", Review of Scientific Instruments, Vol. 75, No. 2, 2004, pp. 515-523

18. Kunikiyo, Y,, Kimoto, T., Nagao, K., "Suirikigaku", Tokyo, Morikita Shuppan, 1971, Chap. 5, pp. 124-140 (in Japanese)